

---

08 Dec 2023

## Design And Performance Of Fiber-reinforced Shrinkage Compensating Eco-friendly Concrete

Kamran Aghaee

Kamal Khayat

Missouri University of Science and Technology, khayatk@mst.edu

Follow this and additional works at: [https://scholarsmine.mst.edu/civarc\\_enveng\\_facwork](https://scholarsmine.mst.edu/civarc_enveng_facwork)



Part of the [Architectural Engineering Commons](#), and the [Civil and Environmental Engineering Commons](#)

---

### Recommended Citation

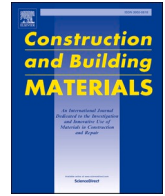
K. Aghaee and K. Khayat, "Design And Performance Of Fiber-reinforced Shrinkage Compensating Eco-friendly Concrete," *Construction and Building Materials*, vol. 408, article no. 133803, Elsevier, Dec 2023. The definitive version is available at <https://doi.org/10.1016/j.conbuildmat.2023.133803>

This Article - Journal is brought to you for free and open access by Scholars' Mine. It has been accepted for inclusion in Civil, Architectural and Environmental Engineering Faculty Research & Creative Works by an authorized administrator of Scholars' Mine. This work is protected by U. S. Copyright Law. Unauthorized use including reproduction for redistribution requires the permission of the copyright holder. For more information, please contact [scholarsmine@mst.edu](mailto:scholarsmine@mst.edu).



Contents lists available at ScienceDirect

# Construction and Building Materials

journal homepage: [www.elsevier.com/locate/conbuildmat](http://www.elsevier.com/locate/conbuildmat)

## Design and performance of fiber-reinforced shrinkage compensating eco-friendly concrete

Kamran Aghaee, Kamal H. Khayat<sup>\*</sup>

Department of Civil, Architectural and Environmental Engineering, Missouri University of Science and Technology, 500 W 16th Street, Rolla, MO 65409, USA

### ARTICLE INFO

#### Keywords:

Ecological and economical concrete  
Expansive agent  
Fiber  
Lightweight sand  
Shrinkage reducing admixture

### ABSTRACT

Eco-Crete is an ecological and economical concrete that benefits from high packing density of solid materials and reduced paste. Eco-Crete can enhance the service life of structures by reducing the risk of shrinkage cracking. In this study, shrinkage mitigating materials included an expansive agent (EA), a shrinkage reducing admixture (SRA), and a lightweight sand (LWS), as well as steel and synthetic fibers were used to minimize the risk of cracking. A total of 35 fiber-reinforced Eco-Crete mixtures were prepared with  $350 \text{ kg/m}^3$  of cementitious materials and 55 % substitution of fly ash and slag. Key fresh and mechanical properties in addition to plastic, restrained, and drying shrinkage were evaluated. Results showed that 32-week drying shrinkage of Eco-Crete made with shrinkage mitigating strategies was limited to  $400 \mu\text{strain}$ , and none of the selected Eco-Crete mixtures experienced cracking up to 112 d under restrained shrinkage testing. Mixtures incorporating only EA and synthetic fibers exhibited excessive initial expansion and minor plastic shrinkage cracking. Eco-Crete mixtures developed at least 40 MPa compressive strength after 56 d. Mixtures made with EA and SRA presented the highest flowability and mechanical properties and the lowest drying shrinkage. The use of synthetic fibers exhibited a better flexural pre-cracking performance than steel fibers. However, steel fiber-reinforced mixtures showed 250 % greater flexural toughness. The use of steel fibers was more effective than synthetic fibers in reducing long-term shrinkage and limiting initial expansion caused by the high content of EA. Statistical analysis and embodied carbon assessment revealed the advantages of using Eco-Crete made with 5 % EA and 0.5 % SRA and 0.5 % synthetic fibers to secure low-shrinkage Eco-Crete.

### 1. Introduction

High-performance concrete (HPC) is commonly proportioned with high content of cementitious materials [1]. The use of high content of cementitious materials and low mixing water in addition to various chemical admixtures in HPC can increase the cost and the vulnerability of HPC to shrinkage cracking [2–4]. Therefore, although the strength is high, the concrete is not economic and service life of the structures made with HPC can be compromised. Ecological and economical concrete (Eco-Crete) is a novel environmentally-friendly concrete, which benefits from low cement content, high replacement content of portland cement by supplementary cementitious materials (SCMs), high packing density of solid particles, and low water-cementitious materials ratio (w/cm) [5–10]. Eco-Crete design seeks limiting the binder volume to about 10 % of the concrete volume.

Optimization of the particle size distribution using the suggested approaches such as optimization curves, particle packing models, and

discrete element modelling [7–9,11,12] leads to higher packing density. Higher packing density reduces the thickness of lubricating layer covering the particles, leading to lower cementitious materials and water demand. The substitution of  $\text{CO}_2$  neutral SCMs and fillers for cement enhances the ecological characteristics and flowability of the concrete. Fennis and Walraven [8] reported that by using a particle packing density approach, concrete mixtures with 50 % lower cement content and 25 % less carbon footprint can be designed. Proske et al. [6] designed and tested an eco-friendly concrete composed of  $90 \text{ kg/m}^3$  cement,  $60 \text{ kg/m}^3$  slag, and  $250 \text{ kg/m}^3$  fly ash (w/cm = 0.36). The authors reported that the mixture can provide adequate workability, 50 MPa compressive strength after 28 d, and equal resistance to long term carbonation compared to the reference mixture made with  $270 \text{ kg/m}^3$  of cement and  $10 \text{ kg/m}^3$  of fly ash. A 35 % reduction in the global warming potential by the substitution of slag and fly ash compared with reference concrete was calculated. While according to the literature [13] the use of 9 to  $14 \text{ kg/m}^3$  binder for earning each MPa compressive strength in

<sup>\*</sup> Corresponding author.

E-mail address: [khayatk@mst.edu](mailto:khayatk@mst.edu) (K.H. Khayat).

<https://doi.org/10.1016/j.conbuildmat.2023.133803>

Received 26 February 2023; Received in revised form 7 October 2023; Accepted 11 October 2023

Available online 18 October 2023

0950-0618/© 2023 Elsevier Ltd. All rights reserved.

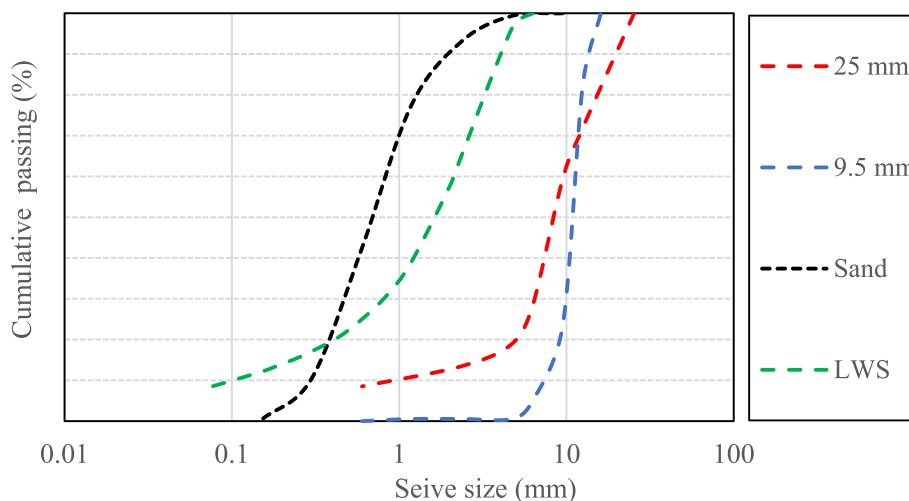
**Table 1**  
Physical and chemical characteristics of cementitious materials.

	Cement	FAC	GGBS	EA
SiO <sub>2</sub> , %	18.7	40.4	36.8	12.6
Al <sub>2</sub> O <sub>3</sub> , %	4.04	19.8	9.2	5.7
Fe <sub>2</sub> O <sub>3</sub> , %	3.56	6.3	0.76	1.9
CaO, %	65.9	24.4	37.1	82.6
MgO, %	1.7	3.5	9.5	0.1
SO <sub>3</sub> , %	2.4	1.0	0.06	–
Na <sub>2</sub> O eq., %	0.97	0.9	–	0.9
Blaine fineness, m <sup>2</sup> /kg	390	490	–	–
Specific gravity	3.14	2.71	2.86	3.12
LOI, %	1.5	–	–	–

conventional concretes is suggested, using packing density, lower w/cm, and high content of SCMs and fillers is expected to promote the mechanical properties and durability of Eco-Crete. Compos et al. [10] reported that using 450 kg/m<sup>3</sup> binder (295 kg/m<sup>3</sup> cement, 64 kg/m<sup>3</sup> silica fume, and 89 kg/m<sup>3</sup> stone powder (a waste material from the limestone sand production process) in concrete proportioned with w/cm of 0.28 can achieve 0.67 packing density, 200 mm slump, and 85 MPa compressive strength after 28 d. Excellent durability based on the ultrasonic pulse velocities (5160 m/s), and negligible corrosion risk (205 KΩcm) for the modified concrete were reported. The low cement and high SCM contents can reduce self-desiccation and autogenous shrinkage [14,15]. The enhanced packing density of the aggregate skeleton can reduce the paste volume and drying shrinkage, and the enhanced packing density of the powder phase can promote impermeability [16–18]. Weng and Liao [19] reported up to 40 % reduction of


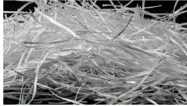

autogenous and drying shrinkage with coupled use of 20 % fly ash and 20 % slag in HPC with 0.34 w/cm owing to the lower water consumption, slower hydration, and microstructure improvement by these SCMs. Lai et al. [20] reported that substituting 35 % of cement with fly ash or limestone filler in concrete with 0.4 w/cm can increase the packing density of the binder phase from 0.850 to 0.863 and 0.864 and reduce the 90-day shrinkage from 690 to 570 and 470 μstrain, respectively. Eco-Crete can also be reinforced with fibers to reduce the risk of cracking and crack widths, hence extending service life [21,22]. Fibers promote Eco-Crete’s performance by providing adequate bond strength and enhancing resistance to shrinkage cracking [23–26]. Arezoumandi et al. [26] utilized 0.3 % micro synthetic fibers in Eco-Crete proportioned with 305 kg/m<sup>3</sup> binder composed of 20 % fly ash, and w/cm of 0.4 to construct large-scale reinforced concrete beams. The beams were examined by four-point bending test, and approximately 5 % higher bonding strength for the fiber-reinforced Eco-Crete beams compared to the reference beam made of conventional concrete with 350 kg/m<sup>3</sup> cement and similar w/cm was observed. Aghaee et al. [24] used 0.5 % hybrid (micro–macro) steel fibers in Eco-Crete (w/cm = 0.4) incorporating 350 kg/m<sup>3</sup> binder that 55 % of cement was substituted by fly ash and slag. The mechanical properties and shrinkage of fiber-reinforced Eco-Crete mixtures subjected to 1 and 14 days of moist curing was compared with the corresponding non-fiber-reinforced Eco-Crete mixtures. The results indicated up to 9 % higher 56 d compressive strength, up to 26 % higher 56 d flexural strength, and 29 % lower shrinkage for both fiber-reinforced Eco-Crete mixtures compared to those of non-fiber-reinforced Eco-Crete mixtures, after 16 weeks.

In addition to the use of packing density, low and alternative binders, and fibers in Eco-Crete, utilizing shrinkage mitigating materials such as



**Fig. 1.** Particle-size distribution of aggregates

**Table 2**  
Physical and mechanical characteristics of fibers.

Fiber Type	Structural synthetic fibers (Type M)	Structural synthetic fibers (Type S)	Structural steel fibers (Type C)
Shape			
Color	Gray	White	Silver
Specific gravity	0.91	0.91	7.85
Length, mm	38	51	60
Aspect ratio	79	74	65
Modulus of elasticity, GPa	–	9.5	200
Tensile strength, MPa	600–650	600–650	1100

**Table 3**  
Mixture proportions of 18 Eco-Crete mixtures (w/cm = 0.4).

Mixture	Cement, kg/ m <sup>3</sup>	FAC, kg/ m <sup>3</sup>	GGBS, kg/ m <sup>3</sup>	Sand, kg/ m <sup>3</sup>	Agg. 25 mm, kg/ m <sup>3</sup>	Agg. 9.5 mm/kg/ m <sup>3</sup>	EA, %	SRA, %	LWS, %	Fiber, %
REF0.5FR (S)	157.5	122.5	70	744	650	465	0	0	0	0.5
10EA0.5FR (M)	142	110	63	744	650	465	10	0	0	0.5
10EA0.25FR (M)										0.25
10EA0.5FR (S)										0.5
10EA0.25FR (S)										0.25
10EA0.35FR (C)										0.35
10EA0.17FR (C)										0.17
5EA0.5SRA0.5FR (M)	150	116	67	744	650	465	5	0.5	0	0.5
5EA0.5SRA0.25FR (M)										0.25
5EA0.5SRA0.5FR (S)										0.5
5EA0.5SRA0.25FR (S)										0.25
5EA0.5SRA0.35FR (C)										0.35
5EA0.5SRA0.17FR (C)										0.17
5EA25LWS0.5FR (M)	150	116	67	570	650	465	5	0	25	0.5
5EA25LWS0.25FR (M)										0.25
5EA25LWS0.5FR (S)										0.5
5EA25LWS0.25FR (S)										0.25
5EA25LWS0.35FR (C)										0.35
5EA25LWS0.17FR (C)										0.17

**Table 4**  
Cracking potential classification adopted from ASTM C1581.

Cracking time, $t_r$ (day)	Average stress rate, $S$ (MPa/day)	Cracking potential
$0 < t_r \leq 7$	$S \geq 0.34$	High
$7 < t_r \leq 14$	$0.17 < S < 0.34$	Moderate – High
$14 < t_r \leq 28$	$0.10 \leq S < 0.14$	Low – Moderate
$t_r > 28$	$S < 0.10$	Low

shrinkage reducing admixtures (SRA), expansive agents (EA), and pre-saturated lightweight sand (LWS) can enhance shrinkage cracking resistance of Eco-Crete [5,27–29]. The SRA decreases surface tension and alkalinity of the pore solution, and restrains the development of autogenous shrinkage [30–33]. Furthermore, SRA lowers the evaporation rate in the matrix and mitigates the drying shrinkage [34–37]. Different types of EAs are commonly used to compensate for shrinkage by initial expansion induced by the formation of ettringite, Ca(OH)<sub>2</sub>, and Mg(OH)<sub>2</sub> platelet crystals in calcium sulfoaluminate (CSA), CaO- and MgO-based EAs, respectively [38–41]. Since high performance concretes are highly impermeable and external water can hardly infuse the matrix, internal curing with porous materials is a promising curing approach [42–46]. Additionally, in the case of using EA in Eco-Crete, adequate water for extending the hydration of EA can be provided by internal curing [47,48]. Using pre-saturated LWS as an internal curing material compensates for the relative humidity drop in matrix and mitigates shrinkage and risk of cracking [24,25,49,73]. Mehdipour and Khayat [5] employed 20 % LWS coupled with 7.5 % CaO-based EA in ecological and economical self-consolidating concrete made with w/cm of 0.45 and 315 kg/m<sup>3</sup> binder (50 % fly ash) and 0.3 % synthetic fibers. The 56 d compressive strength was 28 MPa, drying shrinkage of the concrete was limited to 100  $\mu$ strain, and no cracking was reported after 56 d.

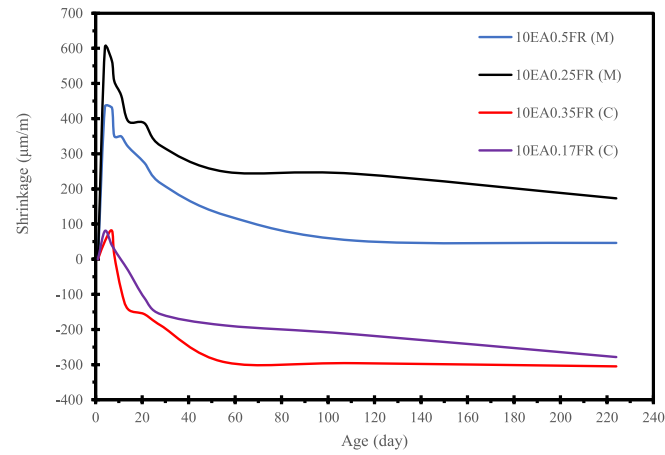
Different approaches such as packing density, use of low paste volume, low w/cm, use of SCMs, and shrinkage mitigating materials can be employed to reduce shrinkage of fiber-reinforced Eco-Crete. Of special interest in this paper is the evaluation of the individual and combined use of EA, SRA, and LWS on eliminating long-term shrinkage and enhancing the crack resistance of fiber-reinforced Eco-Crete that has not been determined in previous studies. This study investigated the

**Table 5**  
Fresh properties of the 18 investigated Eco-Crete mixtures.

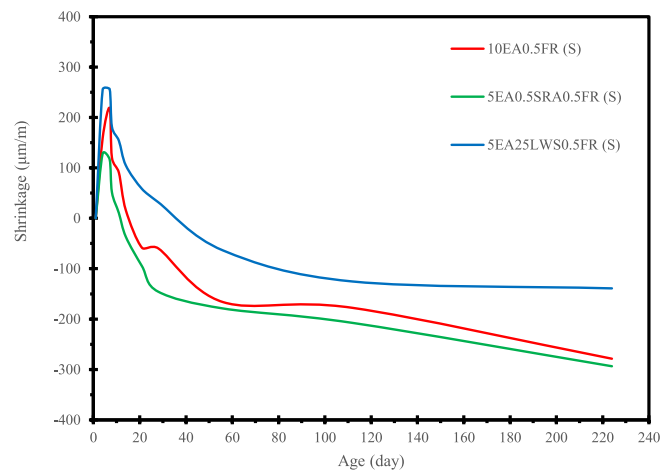
Mixture	Slump, mm	Air content, %	Unit weight, kg/m <sup>3</sup>	HRWR demand, mL/m <sup>3</sup>
REF0.5FR (S)	190	3.5	2444	1170
10EA0.5FR (M)	135	6.0	2330	1170
10EA0.25FR (M)	165	6.5	2323	830
10EA0.5FR (S)	175	6.4	2265	1170
10EA0.25FR (S)	170	6.0	2321	830
10EA0.35FR (C)	200	5.8	2295	850
10EA0.17FR (C)	210	4.8	2285	600
5EA0.5SRA0.5FR (M)	180	3.6	2391	1170
5EA0.5SRA0.25FR (M)	200	6.0	2307	830
5EA0.5SRA0.5FR (S)	160	4.5	2355	1170
5EA0.5SRA0.25FR (S)	195	6.4	2274	830
5EA0.5SRA0.35FR (C)	195	4.2	2423	850
5EA0.5SRA0.17FR (C)	210	5.0	2373	600
5EA25LWS0.5FR (M)	175	4.9	2285	1170
5EA25LWS0.25FR (M)	205	5.3	2249	830
5EA25LWS0.5FR (S)	155	4.7	2307	1170
5EA25LWS0.25FR (S)	195	5.2	2258	830
5EA25LWS0.35FR (C)	210	5.6	2309	850
5EA25LWS0.17FR (C)	195	4.9	2335	600

\*Note: None of the mixtures showed any bleeding.

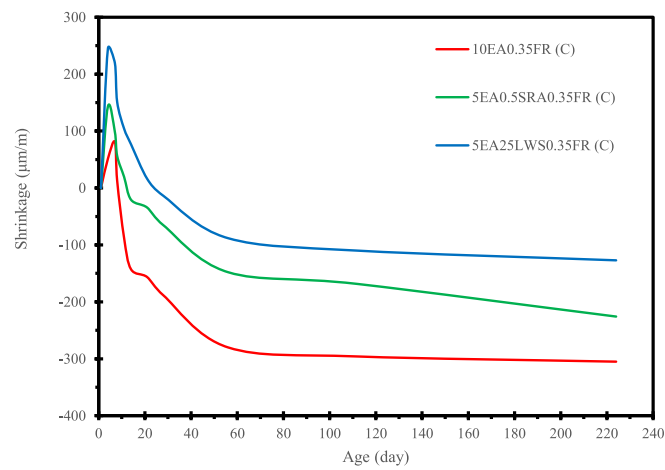
performance of fiber-reinforced Eco-Crete mixtures proportioned with w/cm of 0.4 and 350 kg/m<sup>3</sup> cementitious materials made with individual and combined shrinkage mitigating materials and various fiber types. Key fresh, hardened, and visco-elastic properties were evaluated. Statistical data analysis and embodied carbon assessment of the investigated mixtures were explored to identify optimum Eco-Crete mixtures.



a)



b)



c)

**Fig. 2.** Shrinkage of a) 10EA mixtures reinforced with Types S and C fibers, b) selected mixtures reinforced with Type S, c) selected mixtures reinforced with Type C fibers

**Table 6**  
Shrinkage of Eco-Crete mixture at different ages.

Mixture	Age (day)			
	7	28	112	224
10EA0.5FR (M)	435	215	55	45
10EA0.25FR (M)	565	325	245	175
10EA0.5FR (S)	220	-60	-180	-280
10EA0.25FR (S)	50	-290	-400	-415
10EA0.35FR (C)	80	-190	-295	-305
10EA0.17FR (C)	40	-155	-215	-280
5EA0.5SRA0.5FR (M)	55	-165	-265	-270
5EA0.5SRA0.25FR (M)	50	-180	-270	-305
5EA0.5SRA0.5FR (S)	115	-145	-210	-295
5EA0.5SRA0.25FR (S)	15	-145	-255	-290
5EA0.5SRA0.35FR (C)	100	-65	-170	-225
5EA0.5SRA0.17FR (C)	65	-150	-200	-265
5EA25LWS0.5FR (M)	190	-50	-140	-205
5EA25LWS0.25FR (M)	210	-95	-210	-260
5EA25LWS0.5FR (S)	255	30	-125	-140
5EA25LWS0.25FR (S)	40	-145	-315	-350
5EA25LWS0.35FR (C)	220	-15	-110	-125
5EA25LWS0.17FR (C)	300	70	-30	-50

**Table 7**  
Plastic shrinkage test results on Eco-Crete mixtures.

Mixture	Number of cracks	Crack width, mm	Crack length, mm	Crack density, %
REF0.5FR (S)	0	-	-	0
10EA0.5FR (S)	23	0.05 to 0.3	10 to 165	0.0077
5EA0.5SRA0.5FR (S)	0	-	-	0
5EA25LWS0.5FR (S)	0	-	-	0

**2. Experimental program**

**2.1. Materials**

**2.1.1. Cementitious materials**

A Type I/II cement was used. Class C fly ash (FAC) and ground granulated blast-furnace slag (GGBS) were employed as SCMs. A CaO-

based EA was used to compensate for drying shrinkage by the initial expansion due to the hydration of CaO and formation of portlandite (Ca(OH)<sub>2</sub>). Table 1 presents the physical and chemical properties of the cementitious materials.

**2.1.2. Admixtures**

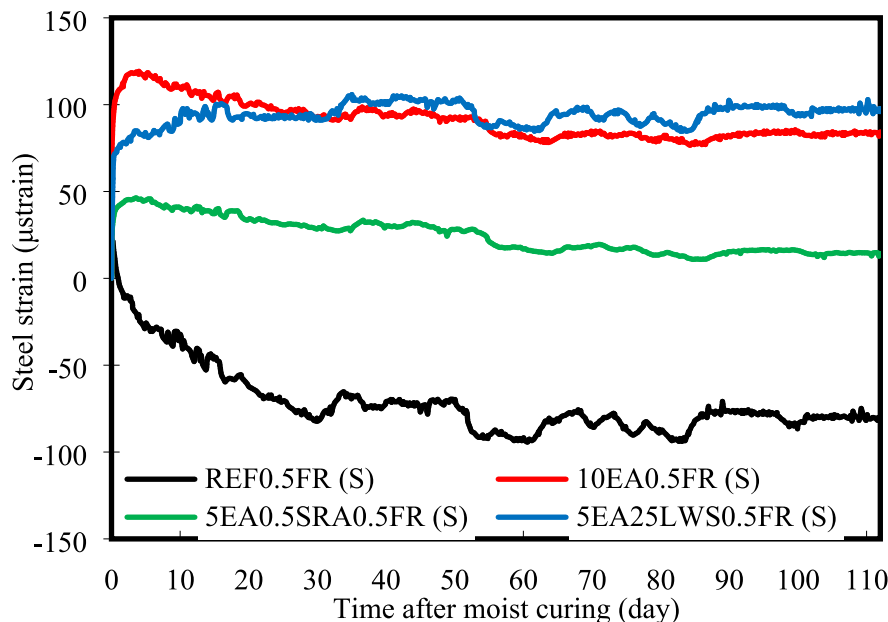
A polycarboxylate-based high-range water reducer (HRWR) with good workability refinement was used. An aqueous solution of highly purified vinsol resin type air entraining agent (AEA) was incorporated to improve the air void system. An SRA was used to mitigate shrinkage. The HRWR, AEA, and SRA had 23 %, 12.5 %, and 15 % solid contents, respectively. The specific gravities of the HRWR, AEA, and SRA are 1.05, 1.01, and 1.002, respectively.

**2.1.3. Aggregates**

Continuously graded natural sand with fineness modulus of 2.60, specific gravity of 2.61, and saturated surface dry (SSD) water absorption value of 0.36 % was used in this study. Pre-saturated expanded shale LWS with a fineness modulus of 3.17 and SSD specific gravity of 1.83 was utilized for internal curing. The LWS water absorption and desorption, were 23.5 %, and 70.3 %, respectively, that were measured according to ASTM C128 and ASTM C1761. Crushed limestone aggregates with a nominal maximum aggregate size of 9.5 and 25.4 mm were used. The specific gravities of aggregates are 2.51 and 2.72, respectively, and their water absorption were 1.16 % and 1 %, respectively. Fig. 1 shows the particle size distribution of the aggregates.

**Table 8**  
Cracking potential classification adopted from ASTM C1581.

Mixture	Cracking time, t <sub>r</sub> (day)	Average stress rate, S (MPa/day)	Cracking potential
REF0.5FR (S)	N.A.	S = 0.003 << 0.10	Low
10EA0.5FR (S)	N.A.	S = 0.003 << 0.10	Low
5EA0.5SRA0.5FR (S)	N.A.	S = 0.0004 << 0.10	Low
5EA25LWS0.5FR (S)	N.A.	S = 0.003 << 0.10	Low



**Fig. 3.** Restrained shrinkage of selected Eco-Crete mixtures made with Type S fibers

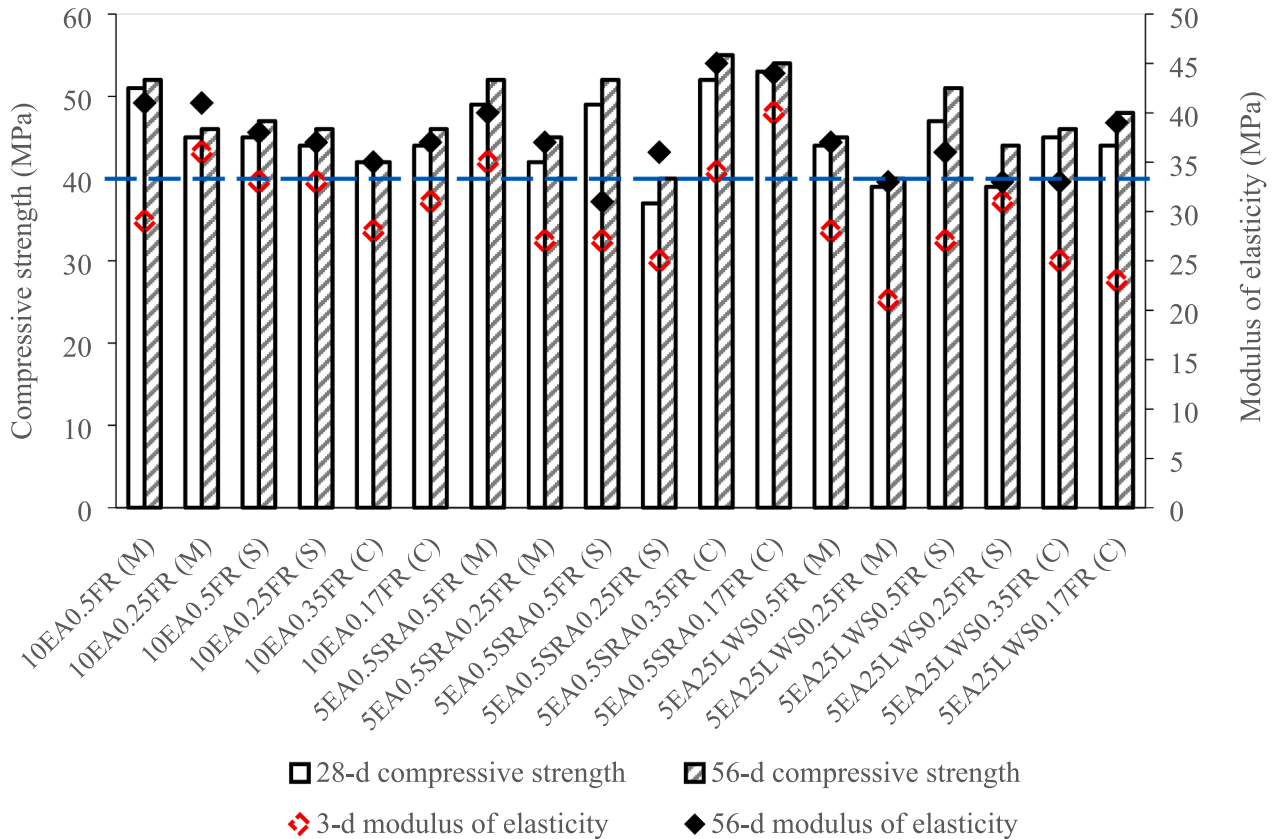


Fig. 4. Compressive strength and modulus of elasticity of the 10EA, 5EA0.5SRA, and 5EA25LWS FRSCC mixtures

#### 2.1.4. Fibers

As shown in Table 2, different types of structural macro steel and synthetic fibers, which are macro copolymer (polypropylene and polyethylene) fibers, were employed. To evaluate the characteristics of different types of fibers on Eco-Crete mixtures, low and moderate contents (0.25 % and 0.5 % for synthetic fibers, 0.17 % and 0.35 % for the steel fiber) were utilized. Table 2 presents the physical and mechanical characteristics of the structural synthetic and steel fibers. The structural synthetic and steel fibers, which were incorporated based on the volumetric fraction of concrete are denoted as Type M, Type S, and Type C fibers throughout this article.

#### 2.2. Mixture proportioning

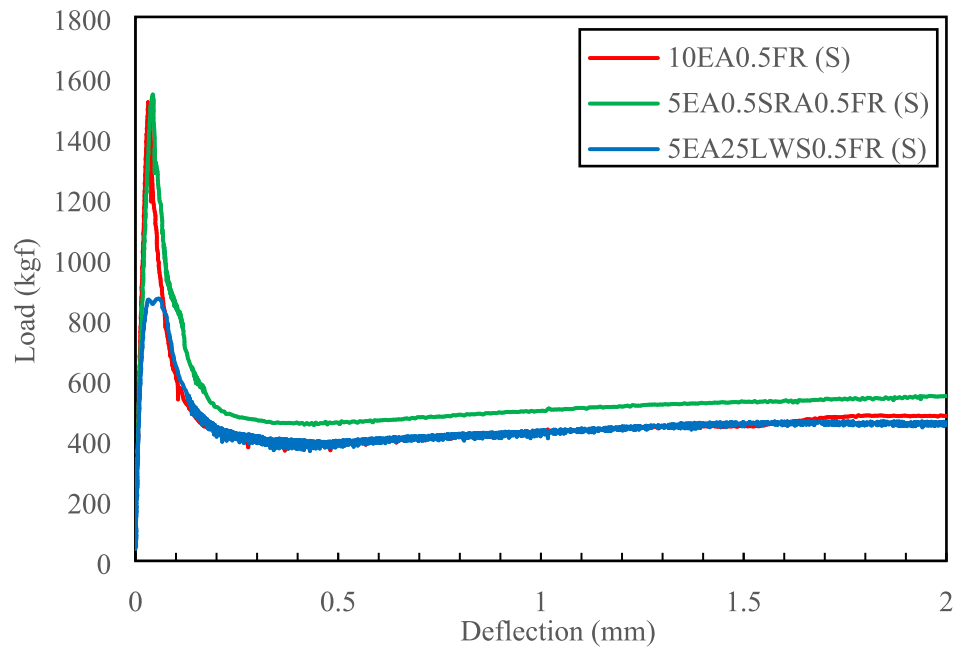
A total of 18 mixtures made with single (EA) and binary combinations (EA-SRA and EA-LWS) of shrinkage mitigating materials were examined. Table 3 presents the mixture proportioning of the investigated mixtures. The EA and SRA were incorporated at 5 wt.% and 0.5 wt % of cementitious materials; LWS substituted 25 vol% of sand. The content and combinations of shrinkage mitigating materials were selected based on the previous studies by the authors [50–52], and are evaluated statistically and ecologically. The Eco-Crete mixtures in this study are denoted based on the contents of EA, SRA, LWS, and fibers. For example, 5EA25LWS0.17FR (C) refers to the mixture made with EA at a dosage of 5 wt% of cementitious materials, LWS at a dosage of 25 vol%

of natural sand and reinforced with 0.17 vol% Type C fibers. The REF0.5FR is the reference mixture made without any shrinkage mitigating materials and containing 0.5 % Type S synthetic fibers. The w/cm was maintained at 0.40 for all mixtures.

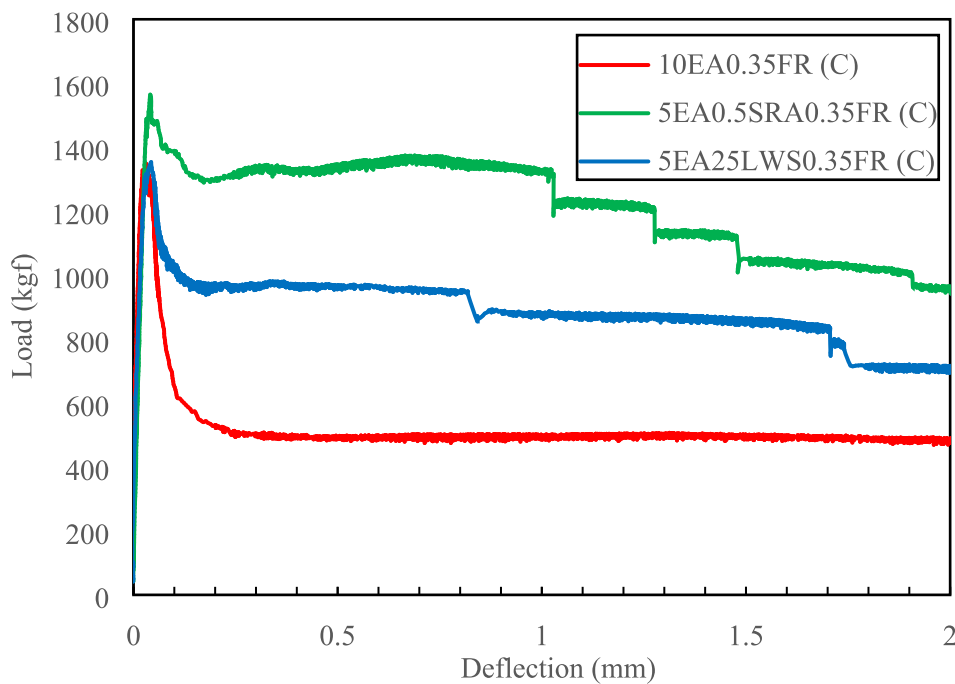
#### 2.3. Mixing and curing procedures

The sand and LWS when applicable was homogenized in mixer for 30 s. This was followed by the addition of the coarse aggregates that were mixed with sand for two minutes. Fibers and half of the water mixed with the AEA were gradually introduced to the mixture. Afterward, the cement, FAC, GGBS, and EA were added and mixed for one minute. Subsequently, the other half of the water mixed with high range water reducer (HRWR) was added and mixing was resumed for four minutes. The mixer was then switched off for two minutes to assess and adjust the flowability of the concrete. The concrete was remixed for an additional two minutes.

All the samples were demolded 24 h after casting and were then subjected to six days of moist curing in lime-saturated water at  $23 \pm 2$  °C. The samples were then transferred to a dry curing chamber with relative humidity and temperature of  $50 \% \pm 4 \%$  and  $23 \pm 2$  °C, respectively.



a)



b)

Fig. 5. Flexural load–deflection curves of the investigated mixtures a) reinforced with Type S and b) Type C fibers

2.4. Testing methods

2.4.1. Fresh properties

2.4.1.1. Slump, density, air content, and bleeding. Testing on fresh properties and sampling of the Eco-Crete mixtures were completed within 15 min from the end of mixing. The slump, unit weight, air

content, and bleeding of the Eco-Crete mixtures were evaluated according to ASTM C143 [53], ASTM C138 [54], ASTM C231 [55], and ASTM C232 [56], respectively.

2.4.2. Visco-elastic properties

2.4.2.1. Plastic shrinkage, drying shrinkage, and restrained shrinkage. The



**Table 9**  
Flexural properties of the 10EA, 5EA0.5SRA, and 5EA25LWS mixtures.

Mixture	Flexural strength, MPa	Deflection at peak load, mm	Residual strength at net deflection of L/600, MPa	Residual strength at net deflection of L/150, MPa	Toughness (area from 0 to L/150), kgf-mm
10EA0.5FR (M)	3.7	0.534	1.3	1.3	731
10EA0.25FR (M)	5.2	0.034	1.1	1.0	657
10EA0.5FR (S)	5.9	0.032	1.5	1.9	937
10EA0.25FR (S)	5.7	0.475	4.2	1.0	800
10EA0.35FR (C)	5.1	0.030	3.1	2.8	1679
10EA0.17FR (C)	4.5	0.030	0.7	0.5	437
5EA0.5SRA0.5FR (M)	6.0	0.043	1.4	1.5	823
5EA0.5SRA0.25FR (M)	4.3	0.024	0.8	0.8	472
5EA0.5SRA0.5FR (S)	5.8	0.044	1.6	2.0	1013
5EA0.5SRA0.25FR (S)	4.7	0.021	0.8	0.8	482
5EA0.5SRA0.35FR (C)	6.1	0.042	5.2	3.7	1984
5EA0.5SRA0.17FR (C)	6.3	0.039	2.3	1.4	1177
5EA25LWS0.5FR (M)	5.1	0.044	1.4	1.5	823
5EA25LWS0.25FR (M)	4.0	0.024	0.7	0.6	423
5EA25LWS0.5FR (S)	4.4	0.036	1.6	1.8	939
5EA25LWS0.25FR (S)	1.8	0.056	1.1	1.1	615
5EA25LWS0.35FR (C)	5.0	0.113	4.0	2.6	1797
5EA25LWS0.17FR (C)	1.8	0.143	1.0	0.9	508

drying shrinkage test was conducted on 75 mm × 75 mm × 285 mm samples according to ASTM C157 [57]. The samples were demolded after 24 h and kept in water tank at 23 ± 2°C up to a week. The samples were then stored in a curing room at constant temperature of 23 ± 2°C and relative humidity of 50 ± 5 %. The volume change was measured using a digital comparator up to 32 weeks, with more frequent readings during the first month.

The plastic shrinkage test was performed on slab samples with dimensions of 560 mm and 350 mm, and a height of 100 mm, in accordance with ASTM C1579 [58]. Two 32 ± 1 mm high stress risers were placed at 90 ± 2 mm inward from each end of the mold at the sides and another one with a height of 64 ± 2 mm at the center of the mold. The concrete was cast in a layer and properly consolidated on a vibrating table. The samples were immediately transferred to a tunnel shape environmental chamber in which the temperature and relative humidity were maintained at 36 ± 3°C and 30 % ± 10 %, respectively. A fan with over 4.7 m/s airflow was placed in the tunnel. Two heat lamps were used to ensure minimum evaporation rate of 1 kg/m<sup>2</sup>.h at 100 ± 5 mm above sample's surface. The experiments were terminated after 24 h, and the number, length, width, and density of plastic shrinkage cracks were then recorded.

The drying shrinkage test was conducted on 75 mm × 75 mm × 285 mm samples according to ASTM C157 [57]. The samples were demolded after 24 h and cured in lime-saturated water at 23 ± 2°C for one week. The samples were then stored in a curing room at 23 ± 2°C and relative humidity of 50 % ± 4 %. The drying shrinkage was measured using a digital comparator up to 32 weeks with frequent readings during the first month of drying.

The restrained shrinkage test was performed on ring samples with external and internal diameters of 405 and 330 mm, respectively, in accordance with ASTM C1581 [59]. Although the maximum size aggregate of Eco-Crete mixtures was 25 mm, the ring test was not performed based on the AASHTO T 334 [60]. concrete ring thickness was 38 ± 1.5 mm and the height was 150 mm. That was done to promote Eco-Crete vulnerability to cracking and accelerate time to cracking. Restraining rings with thickness of 13 mm were used. Two samples were cast for each mixture. The concrete was placed in two layers and each layer was adequately consolidated. Immediately after casting, the

eccentric washers were loosened to not be in contact with the rings. The samples were demolded after 24 h and moist cured using wet burlap covered with plastic sheet up to a week. The samples were then kept in a curing room at constant temperature of 23 ± 2°C and relative humidity of 50 % ± 4 %. Three 120 Ω strain gauges with gauge factors of 2.12 ± 0.5 % were mounted in the interior and at middle height of each steel ring to record the strain of the ring due to the concrete volume change. The strain gauges were connected to a data acquisition system, and the strain measurements were automatically recorded at 20-minute intervals, immediately after casting up to 112 d. The concrete ring samples were visually inspected for crack formation every day. The stress rate of each ring sample at the test termination time was calculated using Eq. (1).

$$q = \frac{G |\alpha_{avg}|}{2\sqrt{t_r}} \quad (1)$$

where q is stress rate (MPa/day), n is day at the test termination time, G is a constant based on the ring dimensions (in this test is 72.2 GPa),  $|\alpha_{avg}|$  is the absolute value of the average strain rate factor [(m/m)/day<sup>0.5</sup>],  $t_r$  is elapsed time at the time of test termination (day).

The average stress rate (S) of the two ring samples was calculated to the nearest 0.01 MPa/day to estimate the cracking potential of the mixtures according to Table 4.

#### 2.4.3. Mechanical properties

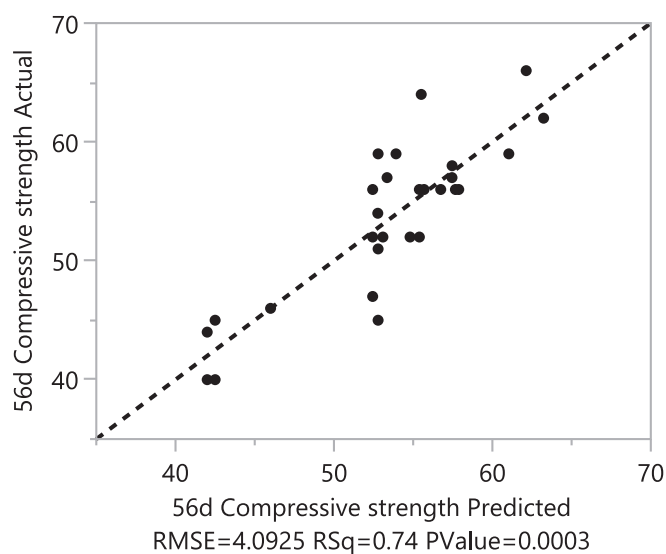
##### 2.4.3.1. Compressive strength, modulus of elasticity, and flexural strength.

The compressive strength tests were conducted on 100 × 200 mm cylinders according to ASTM C39 [61]. The concrete cylinders were ground at the ends before the test to apply a uniformly distributed vertical load according to ASTM C617 [62]. The loading rate was controlled to secure compressive stress of 0.25 ± 0.05 MPa/s.

The modulus of elasticity was performed on 100 × 200 mm cylinders at 3 and 56 d using according to ASTM C469 [63]. The samples were subjected to three cycles of loading and unloading. The testing procedure was set to crosshead travels at a rate of about 1 mm/min. The load rate was maintained to secure compressive stress within the range of

**Table 10**  
56 d compressive strength, 90 d flexural strength, and 224 d shrinkage of the investigated mixtures in statistical analysis.

Mixture	56 d Compressive strength, MPa	90 d Flexural strength, MPa	224 d Shrinkage, $\mu$ strain
10EA0.5FR (M)	52	3.7	46
10EA0.25FR (M)	46	5.2	173
10EA0.5FR (S)	47	5.9	-279
10EA0.25FR (S)	46	5.7	-414
10EA0.35FR (C)	42	5.1	-305
10EA0.17FR (C)	46	4.5	-279
5EA0.5SRA0.5FR (M)	52	6.0	-270
5EA0.5SRA0.25FR (M)	45	4.3	-307
5EA0.5SRA0.5FR (S)	52	5.8	-294
5EA0.5SRA0.25FR (S)	40	4.7	-289
5EA0.5SRA0.35FR (C)	55	6.1	-226
5EA0.5SRA0.17FR (C)	54	6.3	-266
5EA25LWS0.5FR (M)	45	5.1	-205
5EA25LWS0.25FR (M)	40	4.0	-261
5EA25LWS0.5FR (S)	51	4.4	-139
5EA25LWS0.25FR (S)	44	1.8	-349
5EA25LWS0.35FR (C)	46	5.0	-127
5EA25LWS0.17FR (C)	48	1.8	-50
0.5FR (S)	56	-	-215
5EA0.5FR (S)	59	-	-215
10EA0.5FR (S)	56	-	-119
5EA1SRA0.5FR (S)	56	-	-136
5EA2SRA0.5FR (S)	58	-	-170
10EA1SRA0.5FR (S)	54	-	13
10EA2SRA0.5FR (S)	52	-	87
5EA12.5LWS0.5FR (S)	57	-	-225
5EA25LWS0.5FR (S)	59	-	88
10EA12.5LWS0.5FR (S)	56	-	-163
10EA25LWS0.5FR (S)	59	-	-273
5EA1SRA12.5LWS0.5FR (S)	64	-	-197
10EA1SRA12.5LWS0.5FR (S)	57	-	-162
5EA2SRA12.5LWS0.5FR (S)	56	-	-280
5EA2SRA25LWS0.5FR (S)	56	-	-206
10EA1SRA25LWS0.5FR (S)	66	-	-123
10EA2SRA25LWS0.5FR (S)	62	-	-159



**Fig. 6.** Comparison of measured and predicted 56 d compressive strength

250 kPa/s. The specimen was loaded up to 40 % of the average failure load obtained from the compressive strength test. The modulus of elasticity was calculated based on Eq. (2).

$$E = (S_2 - S_1) / (\epsilon_2 - 0.000050) \tag{2}$$

where E is modulus of elasticity per MPa,  $S_2$  is stress corresponding to 40 % of ultimate load,  $S_1$  is stress corresponding to  $\epsilon_1$  (0.000050), and  $\epsilon_2$  is longitudinal strain produced by stress  $S_2$ .

The flexural strength testing was conducted on  $75 \times 100 \times 400$  mm prismatic samples at 90 days according to ASTM C1609 [64]. The loading rate was maintained at displacement control of 0.05 mm/min until the failure. The flexural strength or modulus of rupture was calculated based on Eq. (3).

$$F = PL/bd^2 \tag{3}$$

where, F is the strength (MPa), P is load (N) (testing machine readout + contact load), L is span length (mm) (distance between bottom supports), b is average beam width (mm), and d is average beam depth (mm). The residual loads at deflections of L/600 and L/150 were obtained and the residual strengths calculated. Moreover, toughness which is associated with the ductility of the samples, was achieved by calculating the area under the load–deflection curve up to L/150 displacement.

### 3. Results and discussion

#### 3.1. Fresh properties

Table 5 presents the fresh properties of 18 Eco-Crete mixtures. The slump, air content, and unit weight values were  $170 \pm 40$  mm,  $5 \pm 1.5$  %, and  $2350 \pm 100$  kg/m<sup>3</sup>, respectively. The use of Type M synthetic fibers in 10EA mixture, i.e., 10EA0.5FR (M), led to the lowest slump value, which could be attributed to high water absorption of the EA and synthetic fibers. The hydration caused by the use of relatively high content of EA results in the formation of portlandite and higher specific surface area of compared to cement, which leads to slump reduction [51,52,65]. Higher slump values in the mixtures made with steel fibers, despite the lower HRWR demand, can be related to lower surface area and water absorption of the steel fiber compared to the synthetic fibers [66]. The highest average air content was obtained by the 10EA mixtures, followed by the 5EA25LWS and 5EA0.5SRA mixtures. The synthetic fiber-reinforced mixtures presented higher air content than the steel fiber-reinforced mixtures. As expected, the 5EA25LWS mixtures presented lower unit weight compared to the other mixtures, and synthetic fiber-reinforced mixtures exhibited lower unit weight than the steel fiber-reinforced ones.

#### 3.2. Visco-elastic properties

##### 3.2.1. Drying shrinkage

Fig. 2 and Table 6 present the shrinkage profiles of the Eco-Crete mixtures. The highest 7 d expansion of 565  $\mu$ strain was obtained by the 10EA0.25FR (M) mixture. On average, the highest 7 d expansion was obtained by the 10EA mixtures (230  $\mu$ strain), followed by the 5EA25LWS (205  $\mu$ strain), and 5EA0.5SRA mixtures (65  $\mu$ strain). The higher expansion of the former two mixtures was due to the high content of EA in the 10EA mixture, and the presence of internal curing water coupled with EA in the 5EA25LWS mixture.

The final volume change at 224 d was limited to  $-415$   $\mu$ strain. On average, the lowest shrinkage after 224 d was recorded for the 10EA mixtures ( $-175$   $\mu$ strain), followed by the 5EA25LWS ( $-190$   $\mu$ strain), and 5EA0.5SRA mixtures ( $-275$   $\mu$ strain). On average, the lowest shrinkage during the dry curing (between 7 days and 224 d of age) was recorded for the 5EA0.5SRA mixture ( $-340$   $\mu$ strain), followed by the 5EA25LWS ( $-390$   $\mu$ strain), and 10EA mixtures ( $-410$   $\mu$ strain). Comparing the

**Prediction Profiler (56 d compressive strength)**

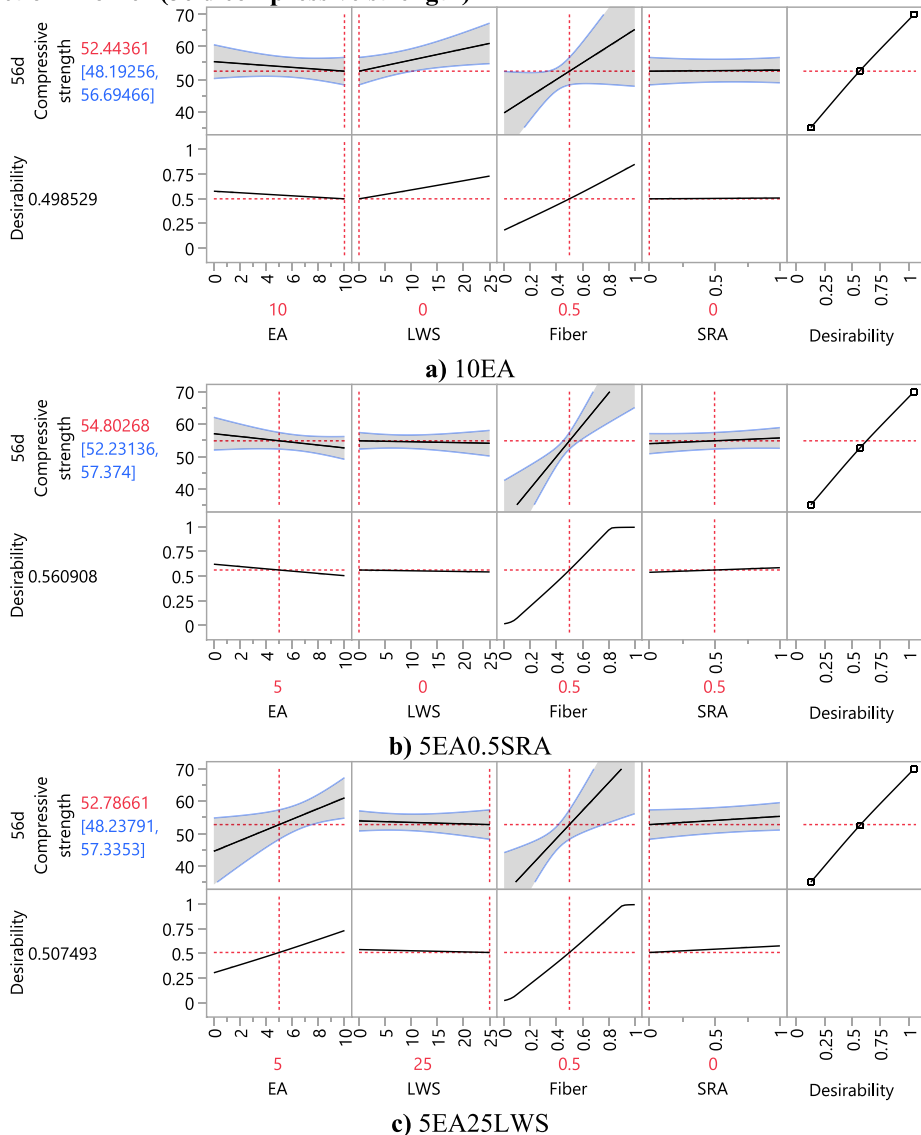


Fig. 7. Prediction profiler of Eco-Crete mixtures for 56 d compressive strength

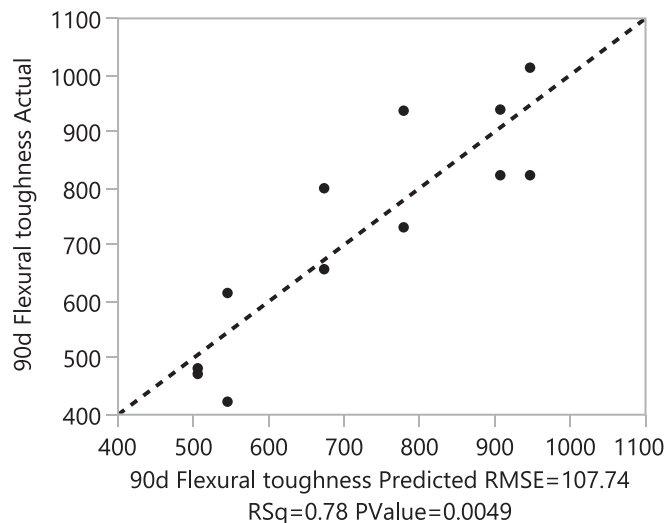


Fig. 8. Comparison of measured and predicted 90 d flexural toughness

average drying and final shrinkage values reveals the importance of high content of EA and moist curing in initial expansion. In addition, the shrinkage mitigating performance of SRA even at low content and in the absence of moist curing is evident.

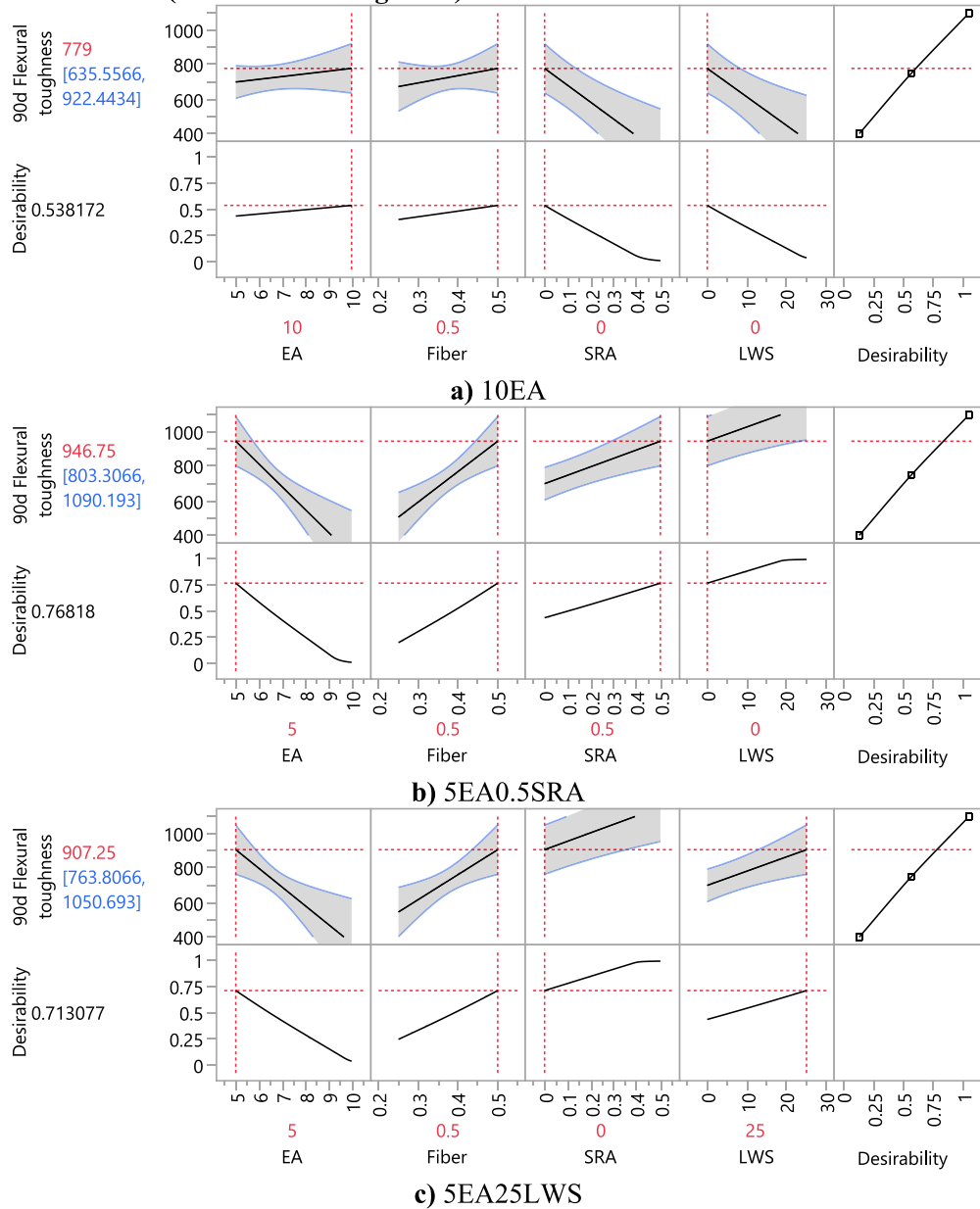
Comparing the effect of fibers on the volume change of the Eco-Crete mixtures, steel fibers were very effective in limiting initial expansion induced by 10 % EA. Limited expansion would reduce the risk of early age cracking, which unless can be induced by excessive expansion of 10 % EA. The steel fibers were also more effective than the synthetic fibers in mitigating drying shrinkage up to 224 d. This can be attributed to the higher modulus of elasticity of the steel fibers compared to the synthetic fibers, as discussed in previous studies [22,67].

The shrinkage profiles of the investigated mixtures show that the effect of the two contents of the steel fibers on shrinkage was insignificant. Therefore, the lower fiber content (0.17 %) can be preferred and applied for restraining volume change.

**3.2.2. Plastic and restrained shrinkage**

Table 7 presents results of the plastic shrinkage on selected Eco-Crete mixtures made with the Type S synthetic fibers. The results show that after the 24-hours duration of the test, only the 10EA0.5FR (S) mixture

**Prediction Profiler (90 d flexural toughness)**



**Fig. 9.** Prediction profiler of Eco-Crete mixtures for 90 d flexural toughness

experienced cracking. The width of the cracks was limited to 0.3 mm, and the crack density was less than 0.01 % of the slab surface. The cracks were not concentrated in the stress riser regions and were spread over the concrete surface. Such cracking can be due to the high content of EA, where the hydration of CaO consumed water and prevented the migration of bleeding water to the concrete surface. Additionally, as discussed in Section 3.2.1 the 10EA mixtures reinforced with synthetic fibers showed excessive early expansion, which confirms plastic shrinkage cracking. The formation of calcium hydroxide crystals by high content of EA induces excessive early-age expansion (Section 3.2.1) that contributes to early age cracking. The use of SRA and LWS coupled with lower content of EA eliminated plastic shrinkage cracking. Such improvement was due to the delaying hydration by SRA and water diffusion by pre-saturated LWS that compensated for the plastic shrinkage [68–70].

The results of the restrained shrinkage testing on selected Eco-Crete mixtures made with Type S synthetic fibers are shown in Fig. 3.

Although the REF0.5FR (S) mixture presented the highest shrinkage, none of the mixtures experienced cracking up to 112 d. The Eco-Crete mixtures did not experience significant volume change after 28 days of testing. The coupled use of EA and SRA caused insignificant expansion shrinkage over the testing time.

The developed stress rate at the test termination time was calculated according to Eq. (1) and cracking potential of the Eco-Crete mixtures was determined, as shown in Table 8. Although the cracking potential of all the mixtures is low (very low), the 5EA0.5SRA0.5FR (S) exhibited the best performance.

**3.3. Mechanical properties**

**3.3.1. Compressive strength and modulus of elasticity**

Fig. 4 displays compressive strength versus modulus of elasticity of the investigated mixtures. The 56 d compressive strength and modulus of elasticity ranged from 40 to 55 MPa and 31 to 45 GPa, respectively.

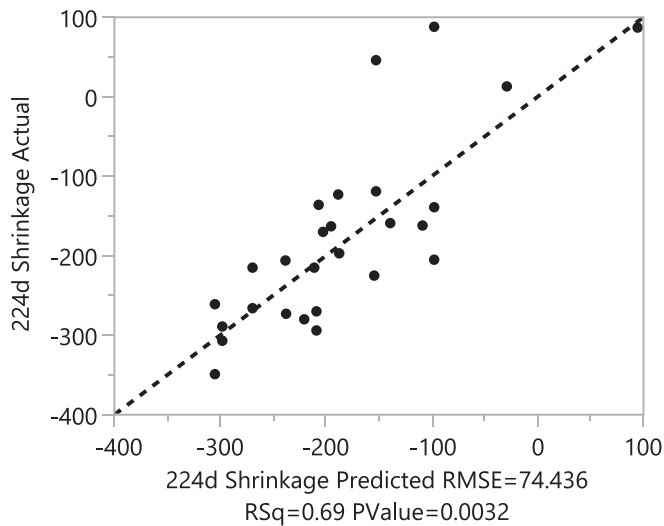


Fig. 10. Comparison of measured and predicted 224 d shrinkage

Using various shrinkage mitigating systems reduced the average 56 d compressive strength of shrinkage compensating Eco-Crete mixtures from 5 % to 12 %. The highest average 56 d compressive strength and modulus of elasticity were exhibited by the 5EA0.5SRA mixture, followed by the 10EA and 5EA25LWS mixtures. The creation of micro cracks and porosity into the matrix due to excessive expansion of 10 % EA led to the strength reduction [51]. Higher mechanical properties were observed using synthetic fibers at the moderate content compared to the low content; the opposite occurred when the steel fiber was used.

### 3.3.2. Flexural strength

Fig. 5 shows flexural load–deflection curves of selected mixtures reinforced with Types S and C fibers at moderate contents. The flexural strength, deflection at first crack, residual strength, and toughness of the mixtures are tabulated in Table 9. The results indicated the better flexural performance of 5EA0.5SRA mixtures compared to the other mixtures. The average flexural strength and deflection upon the first crack of the different shrinkage compensating systems ranged from 3.7 MPa to 5.5 MPa and 0.04 mm to 0.19 mm, respectively. The highest flexural strength and the lowest deflection upon the first crack were recorded for the 5EA0.5SAR mixtures. The 5EA0.5SAR mixtures also presented the highest residual strength and toughness, followed by those of the 10EA and 5EA25LWS mixtures. The synthetic fibers presented a better flexural performance up to the first crack, and on average showed higher flexural strength compared to the steel fiber, while the steel fiber was significantly more effective in post cracking behavior. On average, the flexural toughness values using the steel fiber were nearly two and half times higher than those of the synthetic fibers.

The load–deflection curves shown in Fig. 5 indicate that the moderate content of steel fiber, can provide superior post-cracking performance, followed by the Type S synthetic fiber. The low strength drops especially in the 5EA0.5SAR0.35FR (C) and 5EA25LWS0.35FR (C) mixtures, refers to the proper confinement, cracks bridging, and resistance against the crack propagation by the moderate content of steel fiber [71].

### 3.4. Statistical data analysis

In order to conduct statistical data analysis, an additional 17 mixtures including 0.5 % synthetic fibers with individual, binary, and ternary combinations of the shrinkage mitigating materials at different contents were cast and tested for compressive strength and shrinkage. Table 10 lists the characteristics of the 35 Eco-Crete mixtures, which were used to evaluate the efficacy of the selected shrinkage mitigating

strategies.

A multiple regression analysis of variance was carried out using the least-squares method in JMP software to evaluate the importance of individual and combined effects of the EA, SRA, and LWS on 56 d compressive strength, 90 d flexural strength, and 224 d shrinkage of the Eco-Crete. The statistical significance level, which refers to the probability that a chosen random sample is not representative of the population, was 5 %. Fig. 6 shows the correlation between the actual and predicted 56 d compressive strength values with an  $R^2$  of 0.74.

To better understand the effect of fibers and shrinkage mitigating materials on 56 d compressive strength of Eco-Crete, Eq. (4) (valid for the range of variables considered in this study) was derived from the model.

$$EA + 0.07LWS + 110.8FR + 22.3SRA + 0.08EA \times LWS - 8.5EA \times FR - 1.0LWS \times FR - 0.3EA \times SRA + 0.03LWS \times SRA - 38.1SRA \times FR \quad (4)$$

where, EA is the percentage of EA (% cwt), SRA is the percentage of SRA (% cwt), LWS is the volume percentage of replaced sand by LWS, FR is the volumetric content of synthetic fibers.

The 56 d compressive strength prediction profilers of various shrinkage mitigating strategies, 10EA, 5EA0.5SRA, and 5EA25LWS, are shown in Fig. 7. The prediction profiler graphically illustrates the effect of change in each variable content on a given response (compressive strength, flexural strength, and shrinkage). Desirability numbers correspond to the overall response of the model based on the targeted goal (maximizing, minimizing, or match target), ranged between 0 and 1 were obtained. Higher desirability numbers for a given property reflect a greater performance.

The highest desirability number for the 56 d compressive strength was 0.56 recorded for the 5EA0.5SRA mixtures. The 10EA and 5EA25LWS mixtures had similar desirability numbers of 0.5.

Fig. 8 shows the correlation between the actual and predicted 90 d flexural toughness values with an  $R^2$  of 0.78. The effect of fibers and shrinkage mitigating materials on 90 d flexural toughness of Eco-Crete, is formulated in Eq. (5).

$$726.2 + (EA - 6.7)[(225.1 - 600.2FR) + (FR - 0.375)(395 - 2370SRA) + (LWS - 8.3)(14.9 - 39.8FR)] \quad (5)$$

The 90 d flexural strength prediction profilers of various shrinkage mitigating strategies, 10EA, 5EA0.5SRA, and 5EA25LWS, are shown in Fig. 9. It is observed that the highest desirability number at 0.77 was obtained for the 5EA0.5SRA mixtures. The result of the 90 d flexural strength prediction profilers indicates that the 5EA25LWS and 10EA mixtures presented desirability numbers of 0.71 and 0.54, respectively.

Fig. 10 shows the correlation between the actual and predicted 224 d shrinkage values with an  $R^2$  of 0.69. The effect of fibers and shrinkage mitigating materials on 224 d shrinkage of Eco-Crete, is formulated in Eq. (6).

$$- 77.8EA + 3.0LWS - 538.9FR - 115.3SRA - 1.6EA \times LWS + 178.9EA \times FR + 18.9LWS \times FR + 23.9EA \times SRA - 3.0LWS \times SRA \quad (6)$$

The 224 d shrinkage prediction profilers of various shrinkage mitigating strategies, 10EA, 5EA0.5SRA, and 5EA25LWS, are shown in Fig. 11. It is observed that the highest desirability number at 0.60 was obtained for the 5EA25LWS mixtures. The result of the 224 d shrinkage prediction profilers indicates that the 10EA and 5EA0.5SRA mixtures exhibited desirability numbers of 0.49 and 0.39, respectively.

### 3.5. Embodied carbon

The carbon footprint of the investigated mixtures in this study was

**Prediction Profiler (224 d shrinkage)**

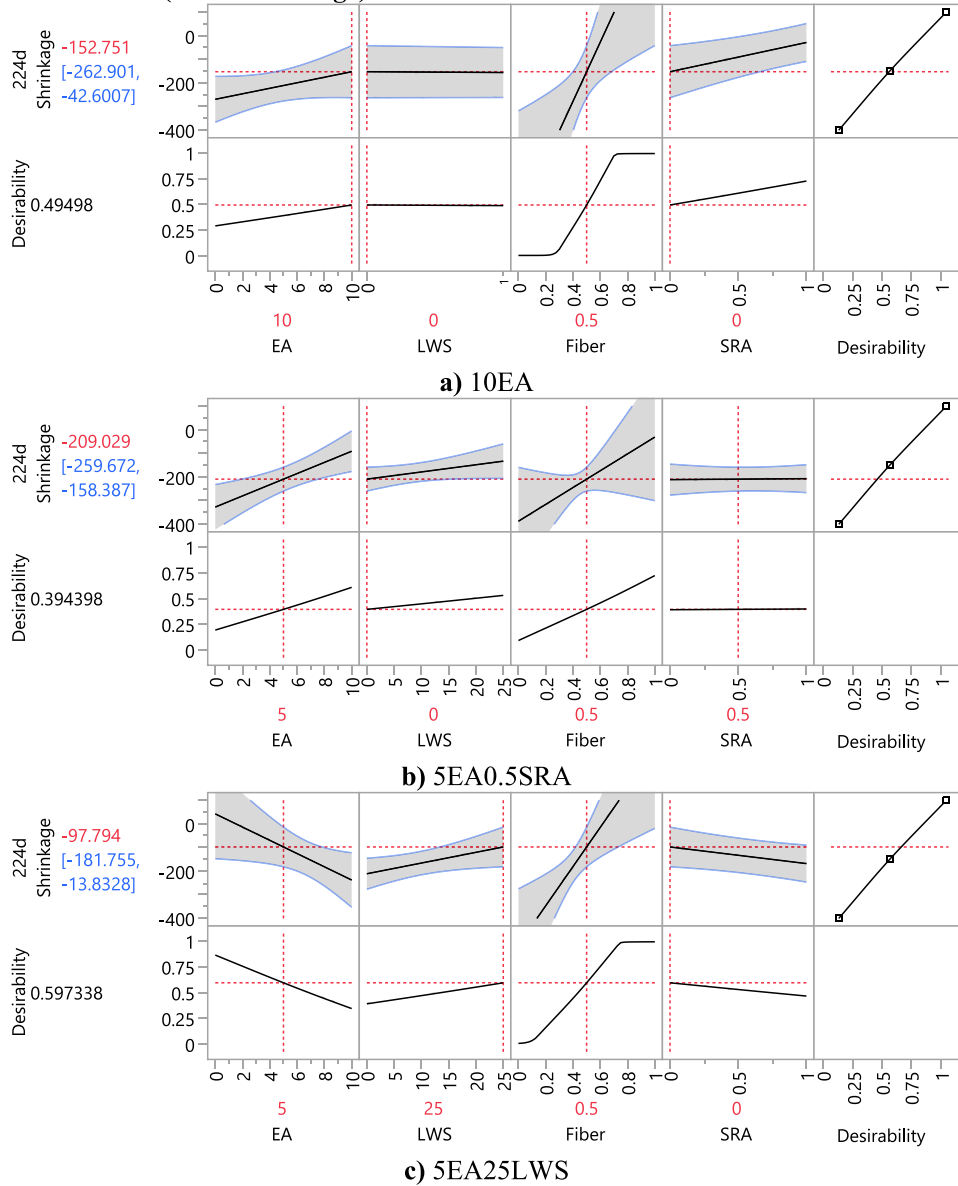


Fig. 11. Prediction profiler of Eco-Crete mixtures for 224 d shrinkage

Table 11

Mixture design of evaluated mixtures for embodied carbon assessment.

Mixture	Cement, kg/m <sup>3</sup>	FAC, kg/m <sup>3</sup>	GGBS, kg/m <sup>3</sup>	Fiber, % (Type)
Mixture 1	350	-	-	0.5 (synthetic)
Mixture 2	157.5	122.5	70	0.35 (steel)
Mixture 3	157.5	122.5	70	0.5 (synthetic)

w/cm = 0.4, HRWR = 1 kg/m<sup>3</sup>, AEA = 0.1 kg/m<sup>3</sup>  
 Total aggregate = 1859 kg/m<sup>3</sup>

analyzed using Concrete Embodied Carbon Footprint Calculator. Three scenarios including a mixture of conventional concrete made of only 350 kg/m<sup>3</sup> cement reinforced with 0.5 % synthetic fibers (Mixture 1), and two Eco-Crete mixtures with similar components to the mixtures investigated in this study reinforced with 0.35 % steel fiber (Mixture 2) and 0.5 % synthetic (Mixture 3) were analyzed. Table 11 presents the mixture design of the investigated mixtures for the embodied carbon assessment.

Fig. 12 and Table 12 present the overall embodied carbon of the

selected mixtures per kg of concrete and the detailed contribution of the mixtures' ingredients in the embodied carbon [72]. It was assumed that the concrete type is in-situ, steel type is world average, and there is no transport from concrete producer to construction site. There is not any steel fiber option in the software, thus the effect of raw steel and hooked end steel fibers used in this study was considered to be similar.

The results revealed that the embodied carbon of Eco-Crete mixtures was up to 49 % lower than the conventional concrete made with only cement and 0.5 % of synthetic fibers. Fig. 12 shows that the mixture incorporating only cement resulted in the highest embodied carbon. The Eco-Crete mixture made with 0.35 % steel fiber rated the second with 37 % lower embodied carbon than the conventional concrete made with only cement and 0.5 % of synthetic fibers. Assuming insignificant embodied carbon by the synthetic fibers (as suggested by the software) the lowest embodied carbon was associated with the Eco-Crete made with 0.5 % synthetic fibers.

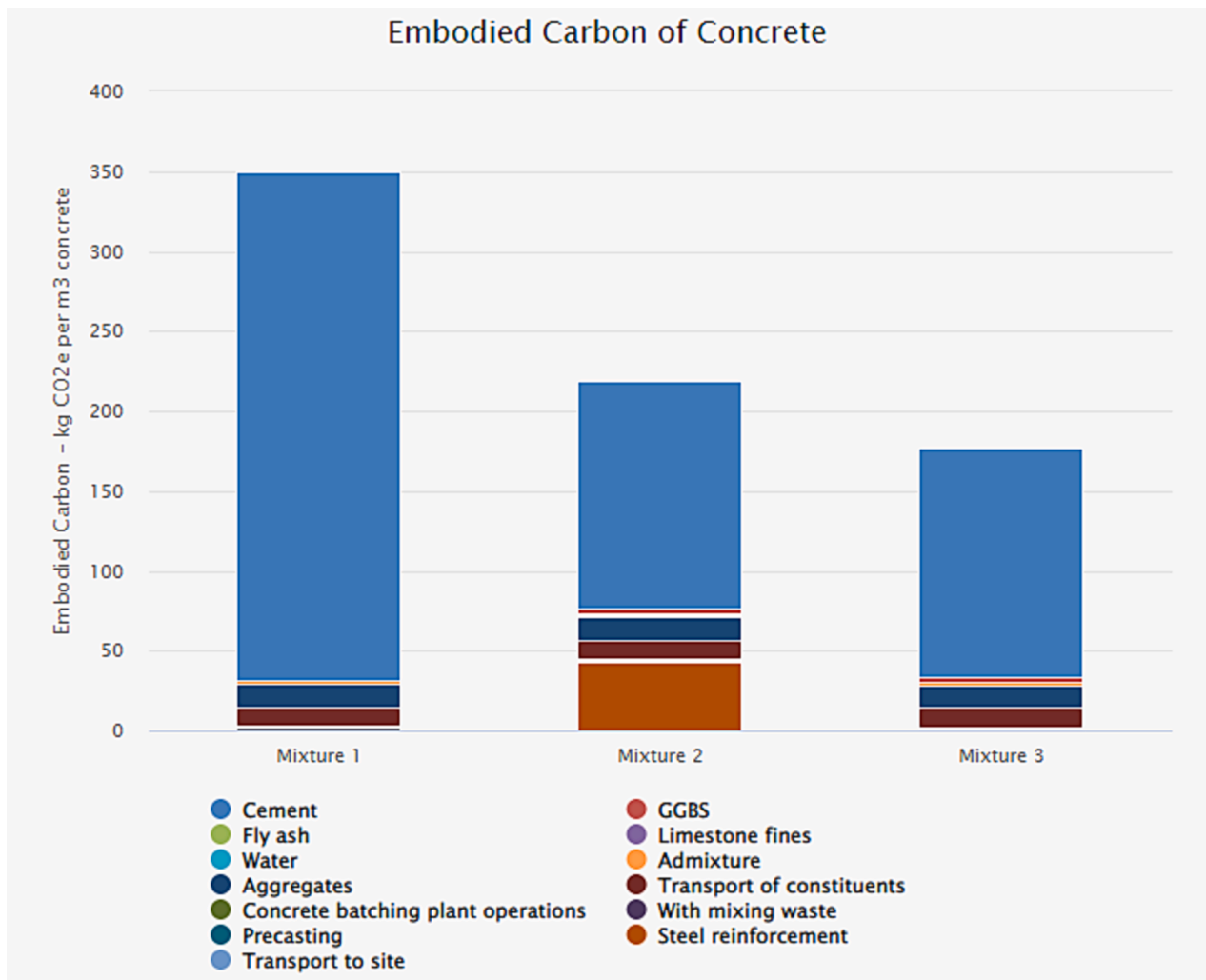


Fig. 12. Comparing embodied carbon of selected mixtures

**Table 12**  
Detailed contribution of mixtures' ingredients and overall estimated embodied carbon of selected mixtures per kg of concrete.

Materials	Mixture 1	Mixture 2	Mixture 3
	Contribution in embodied carbon (%)		
Cement	91.1	65.3	81.1
GGBS	0.0	1.3	1.6
FAC	0.0	0.2	0.3
Admixture	0.6	0.9	1.1
Aggregate	4.0	6.3	7.8
Transport of constituents	3.3	5.3	6.6
Concrete batching plant operations	0.5	0.8	1.0
With mixing waste	0.5	0.4	0.5
Steel reinforcement	0.0	19.4	0.0
kg CO <sub>2</sub> per m <sup>3</sup> concrete	350	219	177
kg CO <sub>2</sub> per kg concrete	0.149	0.093	0.075

#### 4. Conclusions

Shrinkage mitigating strategies using EA, SRA, and LWS and various types of steel and synthetic fibers were employed to enhance the performance of an ecological and economical high-performance concrete (Eco-Crete). Eighteen Eco-Crete mixtures were prepared and tested for fresh properties, mechanical properties, and visco-elastic properties. The following conclusions were drawn.

- Using 10 % EA resulted in the lowest slump due to the hydration and formation of portlandite. Mixtures made with the steel fiber presented lower air content, and higher slump despite of lower HRWR demand compared to those of synthetic fibers due to the lower specific surface area of the steel fibers.
- Various shrinkage mitigating strategies limited the 32-week drying shrinkage of fiber-reinforced Eco-Crete to about 400  $\mu$ strain. Although significant initial expansion was obtained using 10 % EA, the highest and lowest drying shrinkage were recorded for the 10EA and 5EA0.5SRA mixtures, respectively, which indicates the benefit of efficient combination of shrinkage mitigating materials. The steel fiber proved to be more effective than the synthetic fibers in mitigating long-term drying shrinkage.
- Among the selected mixtures subjected to the plastic shrinkage testing, only the 10EA mixture experienced minor cracking (up to 0.3 mm crack width and 0.01 % crack density). Such cracking was due to the presence of high EA content and high moisture demand for the hydration of EA in the corresponding mixture. None of the studied Eco-Crete mixtures subjected to restrained shrinkage test experienced cracking up to 112 d.
- Eco-Crete mixtures secured at least 40 MPa compressive strength. The highest average 56 d compressive strength and modulus of elasticity were obtained by the 5EA0.5SRA mixture. Higher compressive strength and modulus of elasticity were observed using synthetic fibers at the moderate content and steel fiber at low content, which justifies the use of lower content of steel fiber.

- The highest flexural properties presented by the 5EA0.5SAR mixtures. The synthetic fibers presented a better flexural performance until the first crack. However, the flexural toughness values using the steel fiber were nearly two and half times higher than those of the synthetic fibers due to the higher modulus of elasticity and confining effect of the steel fibers.
- The use of Eco-Crete with 55 % SCM and synthetic fibers resulted in 49 % lower embodied carbon production compared to the mixture made without SCM. The results of statistical data analysis and embodied carbon of Eco-Crete mixtures showed that low carbon footprint concrete with adequate mechanical properties and low shrinkage made with 5 % EA and 0.5 % SRA or 5 % EA and 25 % LWS can be produced to be used for bridge and infrastructure construction.

### CRedit authorship contribution statement

**Kamran Aghaee:** Conceptualization, Data curation, Investigation, Formal analysis, Investigation, Methodology, Project administration, Software, Validation, Visualization, Writing – original draft, Writing – review & editing. **Kamal H. Khayat:** Conceptualization, Investigation, Project administration, Resources, Supervision.

### Declaration of Competing Interest

The authors declare that they have no known competing financial interests or personal relationships that could have appeared to influence the work reported in this paper.

### Data availability

Data will be made available on request.

### Acknowledgment

The authors acknowledge the financial support provided by Euclid Chemical (Grant Number: 00064711) and RE-CAST University Transportation Center at Missouri University of Science and Technology (Grant Number: DTRT13-G-UTC45). The valuable cooperation of the Center for Infrastructure Engineering Studies (CIES) and Jason Cox, Senior Research Specialist at the CIES, is greatly appreciated.

### References

- [1] P. Pimienta, R. Jansson McNamee, and J.-C. Mindeguia, Eds., *Physical Properties and Behaviour of High-Performance Concrete at High Temperature: State-of-the-Art Report of the RILEM Technical Committee 227-HPB*, vol. 29. in RILEM State-of-the-Art Reports, vol. 29. Cham: Springer International Publishing, 2019. doi: 10.1007/978-3-319-95432-5.
- [2] L. Wu, N. Farzadnia, C. Shi, Z. Zhang, H. Wang, Autogenous shrinkage of high performance concrete: A review, *Constr. Build. Mater.* 149 (Sep. 2017) 62–75, <https://doi.org/10.1016/j.conbuildmat.2017.05.064>.
- [3] "High Performance Concrete - an overview | ScienceDirect Topics." Accessed: Aug. 23, 2022. [Online]. Available: <https://www.sciencedirect.com/topics/materials-science/high-performance-concrete>.
- [4] I. Ray, Z. Gong, J.F. Davalos, A. Kar, Shrinkage and cracking studies of high performance concrete for bridge decks, *Constr. Build. Mater.* 28 (1) (Mar. 2012) 244–254, <https://doi.org/10.1016/j.conbuildmat.2011.08.066>.
- [5] K. H. Khayat and I. Mehdipour, "Design and Performance of Crack-Free Environmentally Friendly Concrete 'Crack-Free Eco-Crete,'" Art. no. NUTC R322, Aug. 2014, Accessed: Mar. 13, 2020. [Online]. Available: <https://trid.trb.org/view/1321484>.
- [6] T. Prose, S. Hainer, M. Rezvani, C.-A. Graubner, Eco-friendly concretes with reduced water and cement contents — mix design principles and laboratory tests, *Cem. Concr. Res.* 51 (Sep. 2013) 38–46, <https://doi.org/10.1016/j.cemconres.2013.04.011>.
- [7] S. a. a. M. Fennis, "Design of ecological concrete by particle packing optimization," 2011, Accessed: May 08, 2021. [Online]. Available: <https://repository.tudelft.nl/islandora/object/uuid%3A5a1e445b-36a7-4f27-a89a-d48372d2a45c>.
- [8] S. a. a. M. Fennis and J. C. Walraven, "Using particle packing technology for sustainable concrete mixture design," *Heron*, 57 (2012) 2, 2012, Accessed: Aug. 27, 2022. [Online]. Available: <https://repository.tudelft.nl/islandora/object/uuid%3A93af1749-0b97-416a-ba27-907ae4921a7f>.
- [9] P. Ballieu, "Design of ecological concrete by particle packing optimization."
- [10] H. F. Campos, N. S. Klein, and J. Marques Filho, "Proposed mix design method for sustainable high-strength concrete using particle packing optimization," *Journal of cleaner production*, 2020, Accessed: Aug. 27, 2022. [Online]. Available: <https://dx.doi.org/10.1016/j.jclepro.2020.121907>.
- [11] F. D. Larrard, *Concrete Mixture Proportioning: A Scientific Approach*. London: CRC Press, 2014. doi: 10.1201/9781482272055.
- [12] P. Range and L. Lohaus, "Robustness by Mix Design – A New Approach for Mixture Proportioning of SCC," in *Design, Production and Placement of Self-Consolidating Concrete*, K. H. Khayat and D. Feys, Eds., in RILEM Bookseries. Dordrecht: Springer Netherlands, 2010, pp. 37–49. doi: 10.1007/978-90-481-9664-7\_4.
- [13] M.T. de Grazia, L.F.M. Sanchez, R.C.O. Romano, R.G. Pileggi, Investigation of the use of continuous particle packing models (PPMs) on the fresh and hardened properties of low-cement concrete (LCC) systems, *Constr. Build. Mater.* 195 (Jan. 2019) 524–536, <https://doi.org/10.1016/j.conbuildmat.2018.11.051>.
- [14] S.-J. Kim, K.-H. Yang, G.-D. Moon, Hydration characteristics of low-heat cement substituted by fly ash and limestone powder, *Mat. (basel)* 8 (9) (Sep. 2015) 5847–5861, <https://doi.org/10.3390/ma8095277>.
- [15] B. Klemczak, M. Batog, Heat of hydration of low-clinker cements, *J. Therm. Anal. Calorim.* 123 (2) (Feb. 2016) 1351–1360, <https://doi.org/10.1007/s10973-015-4782-y>.
- [16] F. Bustos, P. Martinez, C. Videla, M. Lopez, Reducing concrete permeability by using natural pozzolans and reduced aggregate-to-pasteratio, *J. Civ. Eng. Manag.* 21 (2) (Feb. 2015) 165–176, <https://doi.org/10.3846/13923730.2013.802719>.
- [17] A. A. Ramezani-pour, S. M. Motahari Karein, P. Vosoughi, A. Pilvar, S. Isapour, and F. Moodi, "Effects of calcined perlite powder as a SCM on the strength and permeability of concrete," *Construction and Building Materials*, vol. 66, pp. 222–228, Sep. 2014, doi: 10.1016/j.conbuildmat.2014.05.086.
- [18] R. Saleh Ahari, T. K. Erdem, and K. Ramyar, "Permeability properties of self-consolidating concrete containing various supplementary cementitious materials," *Construction and Building Materials*, vol. 79, pp. 326–336, Mar. 2015, doi: 10.1016/j.conbuildmat.2015.01.053.
- [19] J.-R. Weng, W.-C. Liao, Microstructure and shrinkage behavior of high-performance concrete containing supplementary cementitious materials, *Constr. Build. Mater.* 308 (Nov. 2021), 125045, <https://doi.org/10.1016/j.conbuildmat.2021.125045>.
- [20] M.H. Lai, et al., Shrinkage design model of concrete incorporating wet packing density, *Constr. Build. Mater.* 280 (Apr. 2021), 122448, <https://doi.org/10.1016/j.conbuildmat.2021.122448>.
- [21] A. Sadr-momtazi, S.H. Gashti, B. Tahmouresi, Residual strength and microstructure of fiber reinforced self-compacting concrete exposed to high temperatures, *Constr. Build. Mater.* 230 (Jan. 2020), 116969, <https://doi.org/10.1016/j.conbuildmat.2019.116969>.
- [22] B. Tahmouresi, M. Koushkbaghi, M. Monazami, M.T. Abbasi, P. Nemati, Experimental and statistical analysis of hybrid-fiber-reinforced recycled aggregate concrete, *Comput. Concr.* 24 (3) (2019) 193–206, <https://doi.org/10.12989/cac.2019.24.3.193>.
- [23] I. Mehdipour, K.H. Khayat, Enhancing the performance of calcium sulfoaluminate blended cements with shrinkage reducing admixture or lightweight sand, *Cem. Concr. Compos.* 87 (Mar. 2018) 29–43, <https://doi.org/10.1016/j.cemconcomp.2017.12.001>.
- [24] K. Aghaee, N. Farzadnia, K.H. Khayat, Coupled effect of expansive agent and curing on mechanical and shrinkage properties of fiber-reinforced Eco-Crete, *Constr. Build. Mater.* 310 (Dec. 2021), 125285, <https://doi.org/10.1016/j.conbuildmat.2021.125285>.
- [25] I. Mehdipour, "Characterization and performance of eco and crack-free high-performance concrete for sustainable infrastructure," *Doctoral Dissertations*, Jan. 2017, [Online]. Available: [https://scholarsmine.mst.edu/doctoral\\_dissertations/2581](https://scholarsmine.mst.edu/doctoral_dissertations/2581).
- [26] M. Arezoumandi, D. Garcia, J.S. Volz, Experimental study on bond performance of Eco-Crete and reinforcing steel, *Constr. Build. Mater.* 215 (Aug. 2019) 475–481, <https://doi.org/10.1016/j.conbuildmat.2019.04.253>.
- [27] Mehdipour Iman and Khayat Kamal H., "Elucidating the Role of Supplementary Cementitious Materials on Shrinkage and Restrained-Shrinkage Cracking of Flowable Eco-Concrete," *Journal of Materials in Civil Engineering*, vol. 30, no. 3, p. 04017308, Mar. 2018, doi: 10.1061/(ASCE)MT.1943-5533.0002191.
- [28] K. H. Khayat, I. Mehdipour, and Z. Wu, "Field Implementation and Monitoring of Behavior of Economical and Crack-Free High-Performance Concrete for Pavement and Transportation Infrastructure Constructions – Phase II," p. 69, 2019.
- [29] K. Khayat and I. Mehdipour, "Economic and Crack-Free High-Performance Concrete for Pavement and Transportation Infrastructure Construction | Blurbs New | Blurbs | Main." Accessed: Mar. 16, 2020. [Online]. Available: <http://www.trb.org/Main/Blurbs/176122.aspx>.
- [30] L. Yang, C. Shi, Z. Wu, Mitigation techniques for autogenous shrinkage of ultra-high-performance concrete – a review, *Compos. B Eng.* 178 (Dec. 2019), 107456, <https://doi.org/10.1016/j.compositesb.2019.107456>.
- [31] D.P. Bentz, M.R. Geiker, K.K. Hansen, Shrinkage-reducing admixtures and early-age desiccation in cement pastes and mortars, *Cem. Concr. Res.* 31 (7) (Jul. 2001) 1075–1085, [https://doi.org/10.1016/S0008-8846\(01\)00519-1](https://doi.org/10.1016/S0008-8846(01)00519-1).
- [32] F. Rajabipour, G. Sant, J. Weiss, Interactions between shrinkage reducing admixtures (SRA) and cement paste's pore solution, *Cem. Concr. Res.* 38 (5) (May 2008) 606–615, <https://doi.org/10.1016/j.cemconres.2007.12.005>.



- [33] J. Weiss, P. Lura, F. Rajabipour, G. Sant, Performance of Shrinkage-Reducing Admixtures at Different Humidities and at Early Ages, *ACI Mater. J.* 105 (5) (Oct. 2008) 478–486.
- [34] K.J. Folliard, N.S. Berke, Properties of high-performance concrete containing shrinkage-reducing admixture, *Cem. Concr. Res.* 27 (9) (Sep. 1997) 1357–1364, [https://doi.org/10.1016/S0008-8846\(97\)00135-X](https://doi.org/10.1016/S0008-8846(97)00135-X).
- [35] W.J. Weiss, W. Yang, S.P. Shah, Shrinkage Cracking of restrained concrete slabs, *J. Eng. Mech.* 124 (7) (Jul. 1998) 765–774, [https://doi.org/10.1061/\(ASCE\)0733-9399\(1998\)124:7\(765\)](https://doi.org/10.1061/(ASCE)0733-9399(1998)124:7(765)).
- [36] S.P. Shh, M.E. Krguller, M. Sarigaphuti, Effects of shrinkage-reducing admixtures on restrained shrinkage cracking of concrete, *MJ* 89 (3) (May 1992) 289–295, <https://doi.org/10.14359/2593>.
- [37] K. Aghaee, T. Han, A. Kumar, K.H. Khayat, Mechanism underlying effect of expansive agent and shrinkage reducing admixture on mechanical properties and fiber-matrix bonding of fiber-reinforced mortar, *Cem. Concr. Res.* 172 (Oct. 2023), 107247, <https://doi.org/10.1016/j.cemconres.2023.107247>.
- [38] L. Mo, M. Deng, M. Tang, Effects of calcination condition on expansion property of MgO-type expansive agent used in cement-based materials, *Cem. Concr. Res.* 40 (3) (Mar. 2010) 437–446, <https://doi.org/10.1016/j.cemconres.2009.09.025>.
- [39] “ACI 223-98 Standard Practice for the Use of Shrinkage-Compensating Concrete. Available: <https://library.net/document/y44lpvky-aci-standard-practice-use-shrinkage-compensating-concrete-mycivil.html>.
- [40] L. Mo, M. Deng, and M. Tang, “Effects of Calcination Condition on Expansion Property of MgO-type Expansive Agent Used in Cement-based Materials,” 2010, doi: 10.1016/J.CEMCONRES.2009.09.025.
- [41] S. Nagataki, H. Gomi, Expansive admixtures (mainly ettringite), *Cem. Concr. Compos.* 20 (2) (Jan. 1998) 163–170, [https://doi.org/10.1016/S0958-9465\(97\)00064-4](https://doi.org/10.1016/S0958-9465(97)00064-4).
- [42] P. C. Aitcin, “High Performance Concrete,” CRC Press. Accessed: Mar. 16, 2020. [Online]. Available: <https://www.crcpress.com/High-Performance-Concrete/Aitcin/p/book/9780367865986>.
- [43] H. Al-Khaiat, M.N. Haque, Effect of initial curing on early strength and physical properties of a lightweight concrete, *Cem. Concr. Res.* 28 (6) (Jun. 1998) 859–866, [https://doi.org/10.1016/S0008-8846\(98\)00051-9](https://doi.org/10.1016/S0008-8846(98)00051-9).
- [44] P. Lura, J. Bisschop, On the origin of eigenstresses in lightweight aggregate concrete, *Cem. Concr. Compos.* 26 (5) (Jul. 2004) 445–452, [https://doi.org/10.1016/S0958-9465\(03\)00072-6](https://doi.org/10.1016/S0958-9465(03)00072-6).
- [45] O.M. Jensen, P.F. Hansen, Water-entrained cement-based materials: I. Principles and theoretical background, *Cem. Concr. Res.* 31 (4) (Apr. 2001) 647–654, [https://doi.org/10.1016/S0008-8846\(01\)00463-X](https://doi.org/10.1016/S0008-8846(01)00463-X).
- [46] D. P. Bentz and J. Weiss, “Internal Curing: A 2010 State-of-the-Art Review,” Feb. 2011, Accessed: Mar. 16, 2020. [Online]. Available: <https://www.nist.gov/publications/internal-curing-2010-state-art-review>.
- [47] A.M. Soliman, M.L. Nehdi, Effect of drying conditions on autogenous shrinkage in ultra-high performance concrete at early-age, *Mater. Struct.* 44 (5) (Jun. 2011) 879–899, <https://doi.org/10.1617/s11527-010-9670-0>.
- [48] K. Aghaee, R. Sposito, K.-C. Thienel, K.H. Khayat, Effect of additional water or superplasticizer on key characteristics of cement paste made with superabsorbent polymer and other shrinkage mitigating materials, *Cem. Concr. Compos.* 136 (Feb. 2023), 104893, <https://doi.org/10.1016/j.cemconcomp.2022.104893>.
- [49] K. Aghaee, K.H. Khayat, Effect of internal curing and shrinkage-mitigating materials on microstructural characteristics of fiber-reinforced mortar, *Constr. Build. Mater.* 386 (Jul. 2023), 131527, <https://doi.org/10.1016/j.conbuildmat.2023.131527>.
- [50] K. Aghaee, K.H. Khayat, Effect of shrinkage-mitigating materials on performance of fiber-reinforced concrete – An overview, *Constr. Build. Mater.* 305 (Oct. 2021), 124586, <https://doi.org/10.1016/j.conbuildmat.2021.124586>.
- [51] K. Aghaee and K. H. Khayat, “Benefits and drawbacks of using multiple shrinkage mitigating strategies on performance of fiber-reinforced mortar,” *Cement and Concrete Composites*, p. 104714, Aug. 2022, doi: 10.1016/j.cemconcomp.2022.104714.
- [52] K. Aghaee, R. Sposito, and K. H. Khayat, “Synergistic effect of shrinkage mitigating materials on rheological properties of flowable and thixotropic cement paste,” *Cement and Concrete Composites*, p. 104686, Jul. 2022, doi: 10.1016/j.cemconcomp.2022.104686.
- [53] “ASTM C143 / C143M Standard Test Method for Slump of Hydraulic Cement Concrete – eLearning Course.” Accessed: Aug. 18, 2022. [Online]. Available: <https://www.astm.org/astm-tpt-168.html>.
- [54] “ASTM C138 / C138M Standard Test Method for Density (Unit Weight), Yield, and Air Content (Gravimetric) of Concrete – eLearning Course.” Accessed: Aug. 12, 2022. [Online]. Available: <https://www.astm.org/astm-tpt-192.html>.
- [55] “ASTM C231 / C231M Standard Test Method for Air Content of Freshly Mixed Concrete by the Pressure Method – eLearning Course.” Accessed: Aug. 12, 2022. [Online]. Available: <https://www.astm.org/astm-tpt-171.html>.
- [56] “Standard Test Methods For Bleeding of Concrete ASTM C232/C232M | PDF | Concrete | Water,” Scribd. Accessed: Aug. 18, 2022. [Online]. Available: <https://www.scribd.com/document/353084133/Standard-Test-Methods-for-Bleeding-of-Concrete-ASTM-C232-C232M>.
- [57] Astm, C157, “Test Method for Length Change of Hardened Hydraulic-Cement Mortar and Concrete”, ASTM, International (2017), [https://doi.org/10.1520/C0157\\_C0157M-17](https://doi.org/10.1520/C0157_C0157M-17).
- [58] ASTM C1579, *Standard Test Method for Evaluating Plastic Shrinkage Cracking of Restrained Fiber Reinforced Concrete (Using a Steel Form Insert)*. 2013.
- [59] ASTM C1581, Standard Test Method for Determining Age at Cracking and Induced Tensile Stress Characteristics of Mortar and Concrete under Restrained Shrinkage. ASTM International, West Conshohocken, PA, 2018.
- [60] “AASHTO T 334 - Standard Method of Test for Estimating the Cracking Tendency of Concrete | Engineering360.” Accessed: Sep. 06, 2022. [Online]. Available: <https://standards.globalspec.com/std/2028853/aashto-t-334>.
- [61] ASTM Standard C39, “Test Method for Compressive Strength of Cylindrical Concrete Specimens,” ASTM International, 2018. doi: 10.1520/C0039\_C0039M-18.
- [62] ASTM C 617, “Practice for Capping Cylindrical Concrete Specimens,” ASTM International, 2015. doi: 10.1520/C0617\_C0617M-15.
- [63] ASTM Standard C469, “Test Method for Static Modulus of Elasticity and Poissons Ratio of Concrete in Compression,” ASTM International, 2014. doi: 10.1520/C0469\_C0469M-14.
- [64] “Standard Test Method for Flexural Performance of Fiber-Reinforced Concrete (Using Beam With Third-Point Loading),” ASTM International, 2012. doi: 10.1520/C1609\_C1609M-19A.
- [65] M. Fourmentin, et al., Rheology of lime paste—a comparison with cement paste, *Rheol. Acta* 54 (7) (Jul. 2015) 647–656, <https://doi.org/10.1007/s00397-015-0858-7>.
- [66] V. Guerini, A. Conforti, G. Plizzari, and S. Kawashima, “Influence of Steel and Macro-Synthetic Fibers on Concrete Properties,” *Fibers*, vol. 6, no. 3, Art. no. 3, Sep. 2018, doi: 10.3390/fib6030047.
- [67] V. Corinaldesi, A. Nardinocchi, Influence of type of fibers on the properties of high performance cement-based composites, *Constr. Build. Mater.* 107 (Mar. 2016) 321–331, <https://doi.org/10.1016/j.conbuildmat.2016.01.024>.
- [68] A.E. Naaman, T. Wongtanakitharoen, G. Hauser, Influence of different fibers on plastic shrinkage cracking of concrete, *MJ* 102 (1) (Jan. 2005) 49–58, <https://doi.org/10.14359/14249>.
- [69] R. Henkensiefken, P. Briatka, D. P. Bentz, T. Nantung, and J. Weiss, “Plastic Shrinkage Cracking in Internally Cured Mixtures Made with Pre-wetted Lightweight Aggregate,” vol. 32, no. 2, pp. 49–54, Jan. 2010.
- [70] J. Saliba, E. Rozière, F. Grondin, A. Loukili, Influence of shrinkage-reducing admixtures on plastic and long-term shrinkage, *Cem. Concr. Compos.* 33 (2) (Feb. 2011) 209–217, <https://doi.org/10.1016/j.cemconcomp.2010.10.006>.
- [71] K. Aghaee, M.A. Yazdi, K.D. Tsavdaridis, Investigation into the mechanical properties of structural lightweight concrete reinforced with waste steel wires, *Mag. Concr. Res.* 67 (4) (Feb. 2015) 197–205, <https://doi.org/10.1680/macr.14.00232>.
- [72] “Concrete Embodied Carbon Footprint Calculator,” Circular Ecology. Accessed: Dec. 29, 2022. [Online]. Available: <https://circularecology.com/concrete-embodied-carbon-footprint-calculator.html>.
- [73] K. Aghaee, Synergistic Effect of Shrinkage Mitigating Strategies on Performance of Fiber-Reinforced Cementitious Composites (Doctoral dissertation, Missouri University of Science and Technology), 2022.